JOURNAL OF MATERIALS SCIENCE 27 (1992) 1983–1988

Electrical conductivity of composites: a percolation approach

S. DE BONDT, L. FROYEN, A. DERUYTTERE
Department of Metallurgy and Materials Engineering, Katholieke Universiteit Leuven, B-3001 Heverlee, Belgium

A percolation model has been developed for describing electrical conductivity in particle and short-fibre metal–ceramic composites. Results apply quantitatively to three-dimensional microstructures with fully controlled characteristics (particle shape, orientation and distribution).

1. Introduction

When two powders with different electrical conductivity are mixed, the composite electrical conductivity often appears to be unpredictable in practice. Problems with sintering, pressing, binding agent concentration, porosity, powder oxidation etc. frequently overrule other microstructural characteristics. The influence of these factors not only increases as the powder properties are more and more different, but also as the conductor volume fraction approximates the percolation threshold, p_c (Fig. 1). Since in this zone the electrical conductivity is very dependent on the conductor volume fraction, the factors mentioned seriously hinder experiment interpretation.

2. A percolation model

In order to avoid the experimental problems mentioned, and to be able to predict the position of the percolation threshold in metal–ceramic powder mixtures, a model is introduced. It considers the connectivity of a metallic phase distributed in an insulating phase (steric effects are taken into account only for the metallic phase). The model situates the transition from lower to upper conductivity boundary, as described elsewhere [1–3].

For each type of powder mixture, a series of ten three-dimensional microstructures is developed. This is done by sequentially positioning more and more metal particles in a cubic space of unit size (arbitrary dimensions). A two-dimensional example of this method is given in Fig. 2. In order to obtain physically possible microstructures, the particles are allowed to touch each other only within controlled limits (compare with two-dimensional or overlapping particles considered by others [4–11]). The microstructure is continually being checked for electrical contact between two opposite faces of the cube, chosen perpendicular to the percolation direction. At the end of this procedure, a graphics representation of the microstructure can be produced, as in Fig. 3.

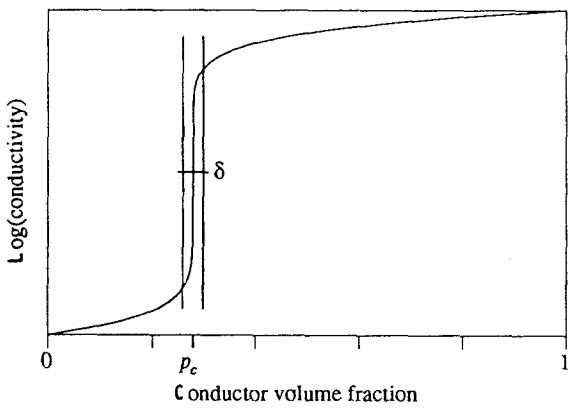

Figure 1 Electrical conductivity versus volume fraction: δ is the transition zone width, p_c is the percolation threshold.

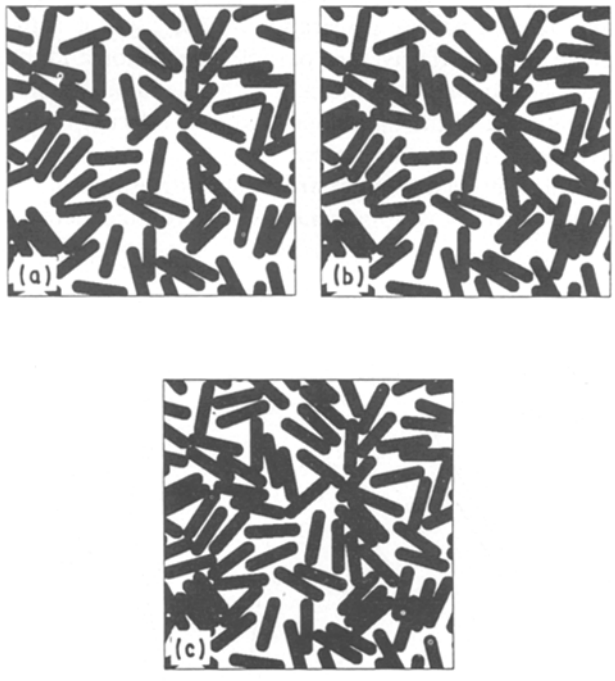

Figure 2 (a–c) Microstructure generation: a two-dimensional example (increasing the conductor volume fraction up to percolation).

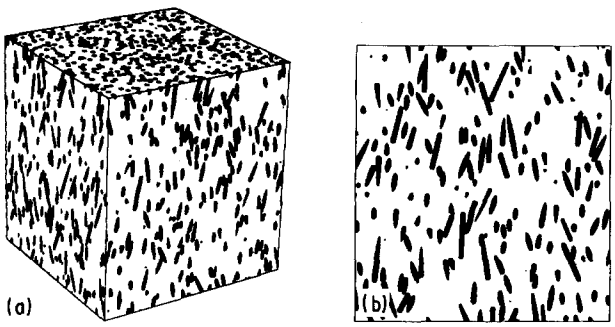

Figure 3 (a) Three-dimensional view and (b) two-dimensional section of a typical microstructure.

In this way, ten volume fractions are calculated. The average is a good estimate for the percolation threshold p_c of the system; the deviation is a measure of the width δ of the percolation transition (Fig. 1). Both these quantities are useful for experiment interpretation.

3. Results

In this section, the influence of some powder characteristics on the percolation volume fraction will be discussed. First, a short notation is introduced for defining powder mixtures.

In the context of the model, a microstructure can most frequently be described by the distribution and characteristics of the metal powder. A two-dimensional example (Fig. 4) illustrates the definitions, with l the particle length and $pp_{a,max}$ the maximal particle penetration. A microstructure is indicated

$$[d, ar, pp_{r,max}, \phi, \alpha_{max}]$$

where d is the particle diameter, ar is the aspect ratio ($= l/d$) (with . . as range-indicator), $pp_{r,max}$ is the maximal relative particle penetration ($= pp_{a,max}/d$), ϕ is the angle between the average particle orientation and the percolation direction and α_{max} is the maximal angular deviation α of the individual particles, referred to the average particle orientation.

Unless otherwise mentioned, the distribution of the metal particles is homogeneous in a volume element with unit size in all three dimensions (arbitrary units), and uniform in spatial orientation deviating from 0 to α_{max} from the average orientation. For all interparticle contacts, the relative particle penetration pp_r should be smaller than $pp_{r,max}$.

3.1. Calculation extent

It is evident that for computer simulations a compromise has to be found between calculation time and accuracy. Smaller particles are equivalent to a larger sample volume (percolation is scale-independent), but also drastically increase the calculation time.

A number of tests have been carried out for one type of microstructure

$$[d, 2..5, 0.125, 0, 30] \qquad 0.032 \leq d \leq 0.1$$

It has been concluded (Fig. 5) that the largest particle dimension should be smaller than a fraction 0.2 of the sample volume dimension. Calculations with this accuracy typically take 1 to 10 h (on a SUN 4/260 computer) per microstructure (i.e. 10 to 100 h for one type of mixture). For even more detailed calculations, results vary only within the width of the transition zone.

3.2. Orientation distribution

For most of the microstructures, the distribution $N(\alpha)$ of metal particles is uniform in spatial orientation, deviating from 0 to α_{max}

$$N(\alpha) \propto \sin\alpha \qquad 0 \leq \alpha \leq \alpha_{max} \qquad (1)$$

This corresponds to Fig. 6. A number of microstructures [11]

[0.04, *ar*, 0.125, 0, 30]	$ar = 2..3, 3..4, 4..5$
[0.02*x*, 4/*x*..10/*x*, 0.25/*x*, 0, 30]	$x = 1, 2, 3$
[0.04, 2..5, 0.125, 0, α_{max}]	$\alpha_{max} = 30, 60, 90$
[0.04, 2..5, 0.125, ϕ, 30]	$\phi = 0, 30, 60, 90$

have also been calculated with a distribution

$$N(\alpha) \propto \sin(\pi\alpha/\alpha_{max}) \qquad 0 \leq \alpha \leq \alpha_{max} \qquad (2)$$

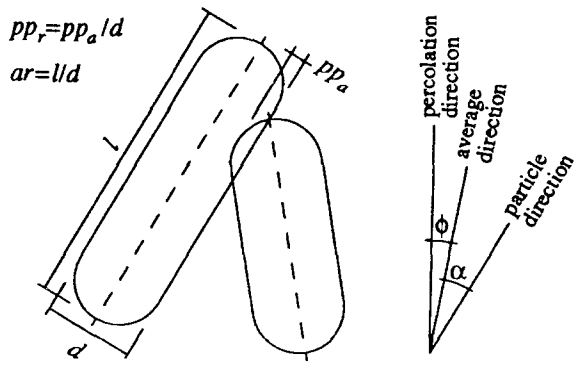

Figure 4 Microstructure characteristics $[d, ar, pp_{r,max}, \phi, \alpha_{max}]$.

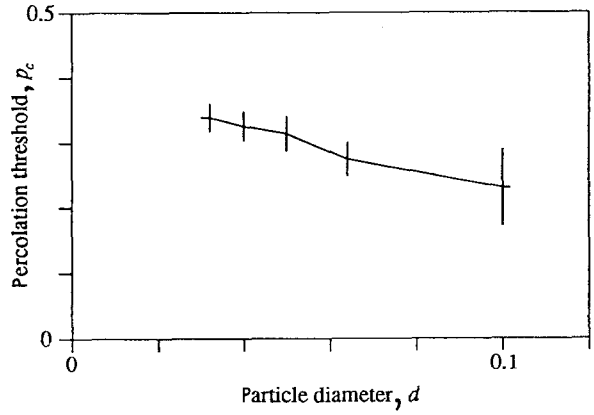

Figure 5 Percolation threshold p_c for different calculation accuracies ($[d, 2..5, 0.125, 0, 30]$ with $0.032 \leq d \leq 0.1$).

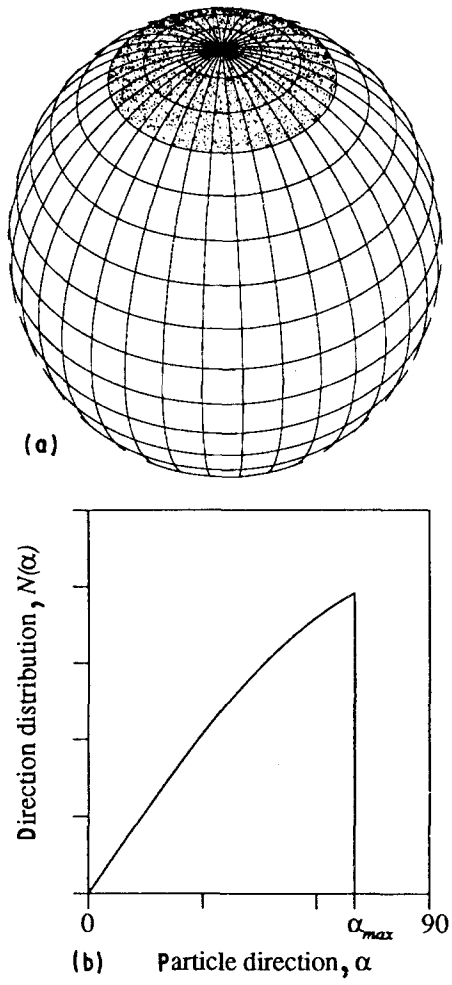

Figure 6 (a, b) Uniform orientation distribution.

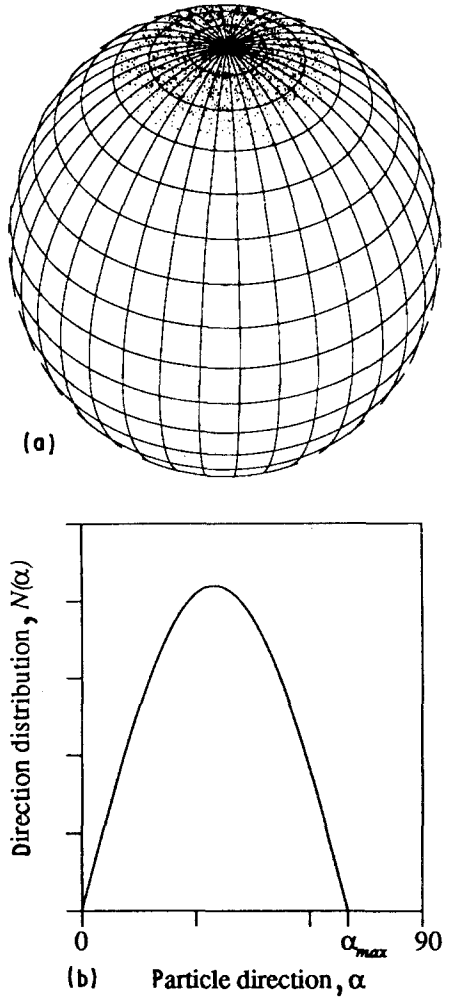

Figure 7 (a, b) Modified orientation distribution.

This corresponds to Fig. 7. From comparison with uniform distribution calculations (microstructures 1 to 11 in Table I and 28 to 38 in Table III), it appears that results are not significantly dependent on the orientation distribution.

3.3. Aspect ratio

The percolation threshold has been determined for aspect ratios from 1 to 10:

[0.2, 1, 0.125, 0, 30]
[0.04, *ar*, 0.125, 0, 30] $ar = 2..3, 3..4, 4..5$
[0.02, 10, 0.125, 0, 30]

Fig. 8 illustrates the dependence of the percolation volume fraction on the metal particle aspect ratio for slightly aligned particles ($\alpha_{max} = 30°$).

3.4. Maximal angular deviation

The smaller the angular deviation from the average orientation, α_{max}, the higher the degree of alignment of the metal particles in the composite. The microstructures investigated are

$[0.04, 2..5, 0.125, 0, \alpha_{max}]$
$\alpha_{max} = 2, 5, 10, 20, 30, 60, 90$

Only for $\alpha_{max} < 10°$ is a slight variation of the percolation threshold observed (Fig. 9). A broadening of the transition zone is also evident in this region.

3.5. Average orientation

The microstructures generated can have an average metal particle orientation different from the percolation orientation. Even for short particles

$[0.04, 2..5, 0.125, \phi, 30]$ $\phi = 0, 30, 60, 90$

a significant increase in percolation volume fraction is observed for perpendicular versus longitudinal percolation (Fig. 10).

4. Discussion

4.1. Factorial analysis

Numerical results in Tables I and III indicate that the percolation volume fraction is very dependent on two microstructural characteristics: the aspect ratio *ar*, and the maximal relative particle penetration $pp_{r,max}$. To quantitatively discuss these influences, Table II has been constructed for microstructures

$[0.04, ar, pp_{r,max}, 0, 30]$

It can be concluded that in the range investigated

TABLE I Uniform orientation distribution

	Microstructure [d, ar, pp_r, ϕ, α_l]	Anisotropy coefficient, Q	Percolation threshold, p_c	Transition width, δ
1	[0.04, 2..3, 0.125, 0, 30]	3.648	0.3448	0.0234
2	[0.04, 3..4, 0.125, 0, 30]	3.858	0.3216	0.0239
3	[0.04, 4..5, 0.125, 0, 30]	3.614	0.2759	0.0397
4	[0.06, 1.33..3.33, 0.083, 0, 30]	3.799	0.3914	0.0192
5	[0.04, 2..5, 0.125, 0, 30]	3.842	0.3256	0.0227
6	[0.02, 4..10, 0.25, 0, 30]	3.847	0.1879	0.0168
7	[0.04, 2..5, 0.125, 0, 90]	1.000	0.3290	0.0251
8	[0.04, 2..5, 0.125, 0, 60]	1.720	0.3151	0.0300
9	[0.04, 2..5, 0.125, 30, 30]	3.841	0.3254	0.0227
10	[0.04, 2..5, 0.125, 60, 30]	3.758	0.3543	0.0270
11	[0.04, 2..5, 0.125, 90, 30]	3.868	0.3680	0.0159
12	[0.1, 2..5, 0.125, 0, 30]	3.687	0.2305	0.0592
13	[0.064, 2..5, 0.125, 0, 30]	3.813	0.2747	0.0262
14	[0.05, 2..5, 0.125, 0, 30]	3.848	0.3141	0.0268
15	[0.032, 2..5, 0.125, 0, 30]	3.808	0.3388	0.0208
16	[0.04, 2..5, 0.125, 0, 20]	5.579	0.3203	0.0312
17	[0.04, 2..5, 0.125, 0, 10]	11.307	0.3429	0.0321
18	[0.04, 2..5, 0.125, 0, 5]	22.711	0.3481	0.0379
19	[0.04, 2..5, 0.125, 0, 2]	57.253	0.3589	0.0432
20	[0.04, 2..5, 0.25, 0, 30]	3.826	0.2435	0.0313
21	[0.04, 4..5, 0.25, 0, 30]	3.780	0.2217	0.0339
22	[0.067, 2..3, 0.25, 0, 30]	3.780	0.2821	0.0125
23	[0.04, 4..5, 0.25, 0, 30]	3.780	0.2217	0.0339
24	[0.067, 2..3, 0.075, 0, 30]	3.876	0.3923	0.0262
25	[0.067, 2..3, 0.15, 0, 30]	3.692	0.3259	0.0253
26	[0.02, 10, 0.125, 0, 30]	3.964	0.2143	0.0311
27	[0.2, 1, 0.125, 0, 0]	3.861	0.3786	0.0298

TABLE II Percolation versus ar and $pp_{r,max}$

ar	$pp_{r,max}$	p_c	Conclusion
2..3	0.125	0.3448	Average = 0.2811
4..5	0.125	0.2759	Factor ar = − 0.0323
2..3	0.25	0.2821	Factor $pp_{r,max}$ = − 0.0292
4..5	0.25	0.2217	Interaction = 0.0021

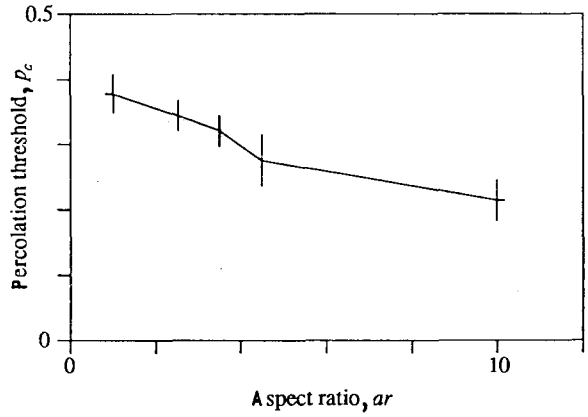

Figure 8 Percolation threshold p_c versus aspect ratio ar.

(i) the interaction between both parameters is negligible (smaller than the deviation of individual results). This proves that they can be treated separately;

(ii) the percolation threshold decreases by ± 3 vol % per unit aspect ratio increase; and

(iii) the percolation threshold p_c decreases by about the same amount when the relative particle penetration is increased by 0.0625.

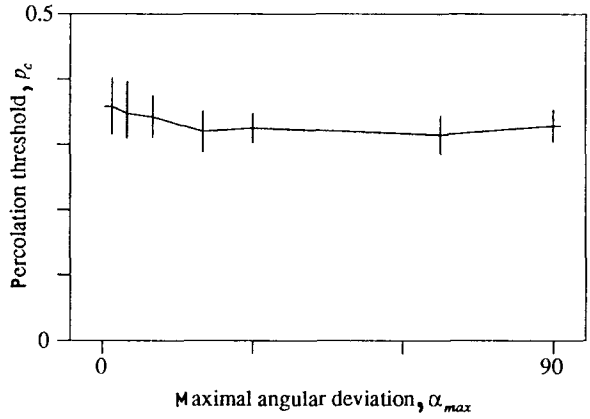

Figure 9 Influence of the maximal angular deviation α_{max}.

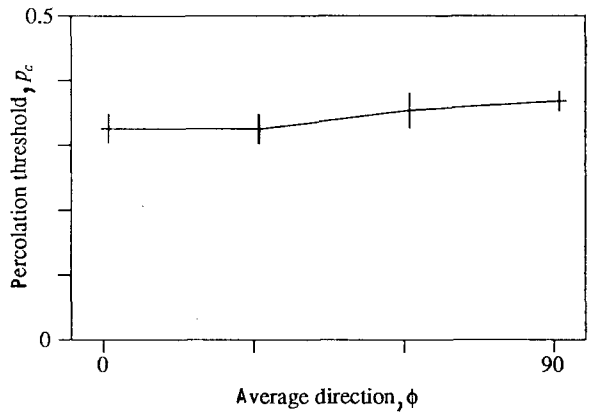

Figure 10 Percolation in different directions ϕ.

TABLE III Modified orientation distribution

	Microstructure [d, ar, pp_r, ϕ, α_l]	Percolation threshold, p_c	Transition width, δ
28	[0.04, 23, 0.125, 0, 30]	0.3287	0.0301
29	[0.04, 34, 0.125, 0, 30]	0.3116	0.0195
30	[0.04, 45, 0.125, 0, 30]	0.2858	0.0220
31	[0.06, 1.333.33, 0.083, 0, 30]	0.3981	0.0269
32	[0.04, 25, 0.125, 0, 30]	0.3383	0.0205
33	[0.02, 410, 0.25, 0, 30]	0.1964	0.0291
34	[0.04, 25, 0.125, 0, 90]	0.3233	0.0185
35	[0.04, 25, 0.125, 0, 60]	0.3124	0.0161
36	[0.04, 25, 0.125, 30, 30]	0.3304	0.0289
37	[0.04, 25, 0.125, 60, 30]	0.3631	0.0310
38	[0.04, 25, 0.125, 90, 30]	0.3753	0.0153

4.2. Usefulness for experiment interpretation

It has been shown that a wide range of percolation volume fractions is covered by the model:

(i) Calculations in the metal particle aspect ratio (ar) interval [1 .. 10] predict volume fractions from 38 to 21 vol %, respectively (section 3.3).

(ii) With maximal relative particle penetrations ($pp_{r,max}$) between 0.075 and 0.25, a percolation threshold from 39 to 19 vol %, respectively, has been found. This microstructural characteristic is related to particle deformation during processing.

(iii) High threshold values are obtained for composites with a metal particle average orientation perpendicular to the percolation direction (section 3.5). In this case the maximal angular deviation is determining.

With the exception of the last case, neither the angular deviation (section 3.4) nor the type of orientation distribution (section 3.2) is important for percolation behaviour.

It has been demonstrated that the model is quite precise in predicting volume fractions. It can be expected, though, that experimental verification will suffer from production-related deviations from the type of microstructure proposed:

(i) the presence of binding agent varies with powder characteristics and volume fraction,

(ii) the presence of other components, reaction or oxidation layers and porosity,

(iii) microstructural characterization in general,

(iv) the number of experiments necessary to determine the percolation threshold.

It is expected that although these problems reduce the absolute quantitative character of the predictions made, the trends discussed will be found in experiments.

4.3. Future extensions

Some research topics are still not covered:

(i) The algorithm of the microstructure generation in the model is easily extendable towards other applications (non-homogeneous distribution of particles, more particle shape statistics, etc.).

(ii) Steric effects between the two phases can be addressed in some cases. One example is briefly introduced: when the metal powder is mixed with a ceramic powder with a fraction of coarse particles, segregation is observed (Fig. 11). It is evident that the percolation volume fraction will be reduced (the volume taken by the coarse ceramic particles is unavailable for the metal particles). On the other hand, the volume fraction relative to the free space for metal particles will increase as the space between ceramic particles becomes more narrow (the packing of particles needs to be more dense, since the percolation path must pass in between the coarse ceramic particles). The example (Fig. 11) contains 54 vol % of coarse ceramic powder. The volume fraction of metal particles relative to free space has been determined for two types of ceramic particle stacking:

[0.06, 1, 0.167, 0, 0]

which for face-centred cubic is 17.9 vol %, and for body-centred cubic 21.1 vol %. The volume fraction for percolation of

[0.06, 1, 0.167, 0, 0]

without coarse ceramic particles is 16.5 vol %.

(iii) The conclusion formulated by Balberg and Binenbaum [8] about anisotropy can be extended to three-dimensional microstructures. It has been attempted to relate the percolation threshold to a set of

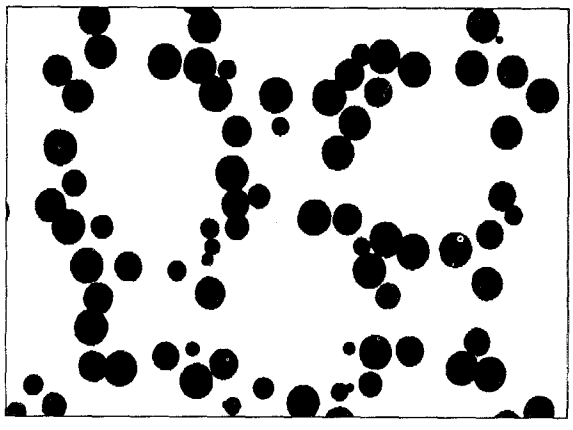

Figure 11 Microstructure with skeleton formation.

anisotropy specifiers: the average particle orientation ϕ, and the generalised anisotropy coefficient

$$Q = \sum l \frac{\cos \alpha}{\sin \alpha} \Big/ \sum l$$

From Tables I and III, which show both specifiers, it is concluded that the extension is not valid. It is suggested that other characteristics be checked for fast percolation volume fraction prediction:

(i) the relative particle penetration,
(ii) the average particle orientation, and
(iii) the volume fraction of particle penetration.

5. Conclusions

A model has been proposed with

(i) fully quantitative calculation of percolation volume fractions in three dimensional microstructures, and

(ii) complete and versatile possibilities for generating and characterising microstructures.

A lot of interpretation and graphic representation facilities have been introduced with respect to experiment control and prediction. Some possible approaches for fast percolation threshold have been formulated.

Acknowledgement

S. De Bondt wishes to thank the National Fund for Scientific Research (Belgium) for his Research Assistant fellowship.

References

1. G. ONDRACEK, in Proceedings, II. Deutsch-Französische Tagung Technische Keramik, Aachen, March 1987, pp. 86–126.
2. D. M. MAGUIRE and F. A. KULACKI, in "Proceedings of 5th International Conference on Composite Materials", ICCM-V, edited by W. C. Harrigan, Jr, J. Strife and A. K. Dhingra, 1985, pp. 1711–1726.
3. D. K. HALE, *J. Mater. Sci.* **11** (1976) 2105.
4. G. E. PIKE and C. H. SEAGER, *Phys. Rev. B* **10** (1974) 1421.
5. N. UEDA and M. TAYA, in "Proceedings of 5th International Conference on Composite Materials", ICCM-V, W. C. Harrigan Jr, J. Strife and A. K. Dhingra, 1985, pp. 1727–1738.
6. M. TAYA and N. UEDA, *Trans. ASME* **109** (1987) 252.
7. N. UEDA and M. TAYA, *J. Appl. Phys.* **60** (1986) 459.
8. I. BALBERG and N. BINENBAUM, *Phys. Rev. B* **28** (1983) 3799.
9. *Idem., Phys. Rev. Lett.* **52** (1984) 1465.
10. C. H. SEAGER and G. E. PIKE, *Phys. Rev. B* **10** (1974) 1435.
11. E. A. HOLM and M. J. CIMA, *J. Amer. Ceram. Soc.* **72** (1989) 303.

Received 20 December 1990
and accepted 13 May 1991